

Phase transition in $\text{ABi}_4\text{Ti}_4\text{O}_{15}$ ($A=\text{Ca}, \text{Sr}, \text{Ba}$) Aurivillius oxides prepared through a soft chemical route

S. K. Rout,^{1,2,a)} E. Sinha,³ A. Hussian,⁴ J. S. Lee,⁴ C. W. Ahn,⁵ I. W. Kim,⁶ and S. I. Woo^{2,b)}

¹Department of Applied Physics, BIT, Mesra, Ranchi, Jharkhand, India

²Department of Chemical and Biomolecular Engineering, KAIST, South Korea

³Department of Physics, NIT, Rourkela, India

⁴School of Materials Science and Engineering, University of Ulsan, South Korea

⁵High Technology Components and Materials Research Center, Busan Center, Korea Basic Science Institute, Busan 618-230, South Korea

⁶Department of Physics, University of Ulsan, South Korea

(Received 21 July 2008; accepted 8 December 2008; published online 23 January 2009)

A series of compounds, $\text{CaBi}_4\text{Ti}_4\text{O}_{15}$ (CBT), $\text{SrBi}_4\text{Ti}_4\text{O}_{15}$ (SBT), and $\text{BaBi}_4\text{Ti}_4\text{O}_{15}$ (BBT), belonging to the Aurivillius-type structure (four layers) has been prepared by a modified chemical route. Different oxalates were precipitated from their respective nitrate solution onto the surface of TiO_2 powders. The room temperature x-ray diffraction study revealed that the compounds were having orthorhombic symmetry. Considering the tolerance factor, a significant deformation of the perovskite block is observed and that decreases with increase in ionic radius of A site atom. Temperature dependent dielectric study showed normal ferroelectric to paraelectric transition well above the room temperature except for BBT. The BBT ceramic showed a relaxorlike behavior near phase transition. The quantitative characterization and comparison of relaxor behavior were based on empirical parameters γ and ΔT_{res} . The dielectric relaxation rate follows the Vogel–Fulcher relation with activation energy=0.02 eV and freezing temperature=362 °C. All these measurements confirmed its relaxorlike phase transition. © 2009 American Institute of Physics. [DOI: 10.1063/1.3068344]

I. INTRODUCTION

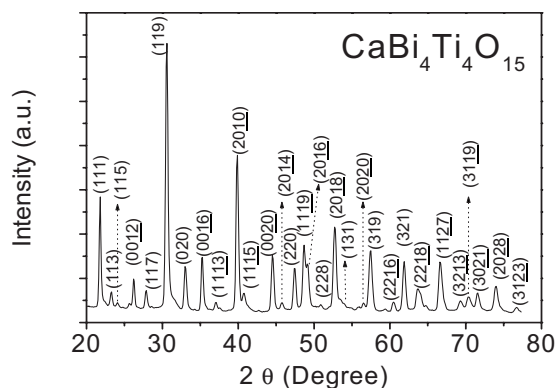
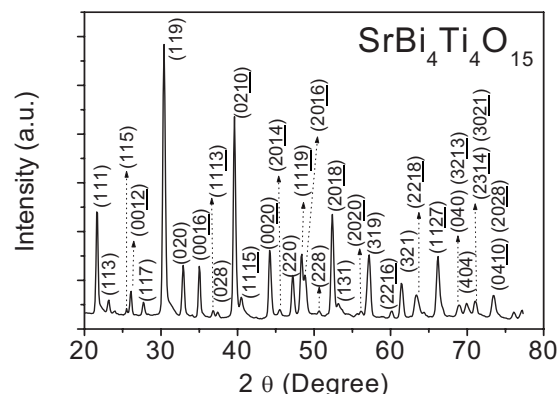
On the basis of structure ferroelectric oxides may be classified into four types: (1) perovskite (e.g., BaTiO_3 , KNbO_3), (2) pyrochlore (e.g., $\text{Cd}_2\text{Nb}_2\text{O}_7$), (3) tungsten bronze (e.g., PbNbO_6 , PbTaO_6), and (4) layer-type bismuth compound (e.g., $\text{PbBi}_2\text{Nb}_2\text{O}_9$). A feature common to all these four structures is the presence of ions of small size and large charge (e.g., Ti^{4+} , Nb^{5+} , Ta^{5+} , etc.) in oxygen octahedra, which are linked through corners forming a continuous chain of oxygen-metal-oxygen. Since bismuth layered structure ferroelectrics play an important role in the dielectric and ferroelectric devices, its crystal structure and material properties have been widely investigated for the past several decades.^{1–3} In its crystal structure perovskite blocks ($A_{m-1}B_m\text{O}_{3m+1}$) are sandwiched between Bi_2O_2 layers and these perovskite blocks are composed of m layer BO_6 octahedra with A site cation. In this notation A represents mono-, bi-, or trivalent ion and B denotes a tetra-, penta-, or hexavalent ion.

Aurivillius oxides, $\text{CaBi}_4\text{Ti}_4\text{O}_{15}$ (CBT), $\text{SrBi}_4\text{Ti}_4\text{O}_{15}$ (SBT), and $\text{BaBi}_4\text{Ti}_4\text{O}_{15}$ (BBT) attracted much attention because of their low operating voltage, fast switching speed, negligible fatigue up to 10^{12} switching cycles, excellent retention characteristics, and low leakage current density on Pt electrodes for integrated device applications in nonvolatile

ferroelectric random access memory (FRAM).^{4–8} Large remnant polarization, low coercive field, and high Curie temperature are required for better performance and reliable operations of FRAM devices. These physical properties of ceramics are greatly affected by the characteristics of the powder, such as particle size, morphology, purity, and chemical composition. Chemical methods, e.g., coprecipitation, sol gel, and hydrothermal and colloid emulsion technique have been confirmed to efficiently control the morphology and chemical composition of prepared product. However, these wet chemical techniques, sol gel, and hydrothermal and colloid emulsions are time consuming and involve highly unstable alkoxides and it is difficult to maintain reaction conditions. Ceramics are usually prepared by grinding and calcinations of oxides and carbonates. However, this method has several disadvantages such as compositional inhomogeneity, nonuniformity of particle size and shape, high impurity content, lack of reproducibility, and necessity of repeating the process. The conventional way to synthesize Bi based layer structure via solid-state reaction at high temperatures⁹ is also not suitable for ferroelectric applications since the high-temperature synthesis can lead to the formation of an unwanted nonferroelectric bismuth-deficient pyrochlore phase resulting from the severe loss of the bismuth component at high temperatures.^{10–12} The soft chemical method presents many advantages, such as the possibility to work with aqueous solution at high stoichiometry control. Cost effectiveness such as low-temperature processing and inexpensive precursors and equipments are some additional advan-

^{a)} Author to whom correspondence should be addressed. Tel.: +91-94370-85441. Electronic mails: skrout@bitmesra.ac.in and drskrout@gmail.com.

^{b)} Electronic mail: siwoo@kaist.ac.kr.

FIG. 1. Room temperature powder XRD pattern of $\text{CaBi}_4\text{Ti}_4\text{O}_{15}$ ceramic.FIG. 2. Room temperature powder XRD pattern of $\text{SrBi}_4\text{Ti}_4\text{O}_{15}$ ceramic.

tages. In the present study, Aurivillius oxides $\text{ABi}_4\text{Ti}_4\text{O}_{15}$ ($A=\text{Ca}, \text{Sr}, \text{Ba}$) ceramics have been prepared by a modified chemical route and their temperature dependent dielectric properties have been investigated. The obtained physical properties were compared with earlier structural reports on these compositions.

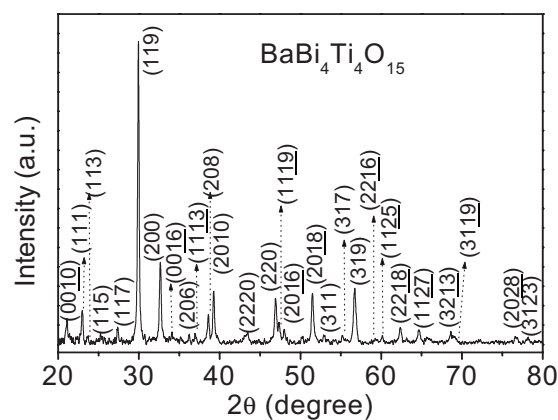
II. EXPERIMENTAL

The basic materials used in the synthesis were $\text{Ca}(\text{NO}_3)_2$, $\text{Sr}(\text{NO}_3)_2$, $\text{Ba}(\text{NO}_3)_2$, $\text{Bi}(\text{NO}_2)_3$, TiO_2 ($d_{10}=0.27 \mu\text{m}$, $d_{50}=0.35 \mu\text{m}$, and $d_{90}=0.48 \mu\text{m}$), and oxalic acid. An aqueous solution of 0.2M of the respective alkaline earth metal nitrate and bismuth nitrate were prepared using de-ionized water. An appropriate amount of TiO_2 was added to a 0.2M oxalic acid solution and was ultrasonicated for 10 min to break TiO_2 agglomeration and then kept on the stirrer for continuous stirring to ensure suspension. The solution containing alkaline earth metal nitrate and bismuth nitrate were added dropwise into the suspension of TiO_2 in oxalic acid solution under continuous stirring. Finally the pH of the solution was maintained at 7 by adding ammonia solution. All of the above experiments were carried out at room temperature. This process precipitates alkaline earth metal oxalate on the surface of fine TiO_2 particles by nucleation. Similar types of ceramic synthesis have been reported earlier by the same author for $\text{BaTi}_{0.6}\text{Zr}_{0.4}\text{O}_3$ (Ref. 13) and BaTiO_3 .¹⁴ The resulting precipitate was filtered out and washed repeatedly with isopropyl alcohol and the powders were calcined at 750 °C for 4 h and 950 °C for 4 h with intermediate mixing and grinding. The synthesized powders were characterized with respect to phase identification and lattice parameter measurements using $\text{Cu K}\alpha$ x-ray diffraction (XRD) (Xpert MPD, Philips). Surface morphologies were studied by using a scanning electron microscope (SEM, S-4200, Hitachi, Japan). For electrical property measurements, pellets were prepared with 2 wt % polyvinyl alcohol solution added as binder and were sintered at 1050 °C for 4 h. The density and porosity were evaluated using Archimedes' principle and found to be nearly 97% of the theoretical density. Silver electrodes were applied on the opposite disk faces by dc sputter (Cressington 108, Cressington, Inc., USA). Dielectric measurements were carried out in the frequency range from 50 Hz to 1 MHz using an imped-

ance analyzer (HP 4192A, USA) connected to a personal computer. The dielectric data were collected at an interval of 2 °C while heating at a rate of 0.5 °C/min.

III. RESULTS AND DISCUSSION

Figures 1–3 show the room temperature powder XRD patterns of CBT, SBT, and BBT ceramics recorded by using $\text{Cu K}\alpha$ radiation. The preparation of Bi layered ceramics is always troubled by the coexistence of a pyrochlore phase, which is considered to be due to the thermal decomposition reaction caused by the vaporization of bismuth species. In the present work, there is no such evidence of the existence of any impurity phase or its quantity is too small to be detected. The XRD patterns were indexed in the orthorhombic symmetry and cell parameters were refined by using the standard CCP-14 program CHEKCELL.¹⁵ The lattice parameters are found to be $a=5.461$, $b=5.4235$, and $c=40.550 \text{ \AA}$ for CBT, $a=5.4507$, $b=5.4376$, and $c=40.9841 \text{ \AA}$ for SBT, and $a=5.443$, $b=5.432$, and $c=41.694 \text{ \AA}$ for BBT ceramic. These observed lattice parameters are in excellent agreement with those reported elsewhere.^{16–18} Aurivillius originally described BBT as tetragonal at room temperature, while remaining oxides (SBT, CBT) as orthorhombic.¹⁹ Irie *et al.*²⁰ suggested that BBT is in fact orthorhombic, although they did not present any detailed structural information. Recently, Kennedy *et al.*²¹ studied the structure of the four oxides $\text{ABi}_4\text{Ti}_4\text{O}_{15}$ ($A=\text{Ca}, \text{Sr}, \text{Ba}, \text{Pb}$) using a combination of powder synchrotron x-ray and neutron diffraction data. They sug-

FIG. 3. Room temperature powder XRD pattern of $\text{BaBi}_4\text{Ti}_4\text{O}_{15}$ ceramic.

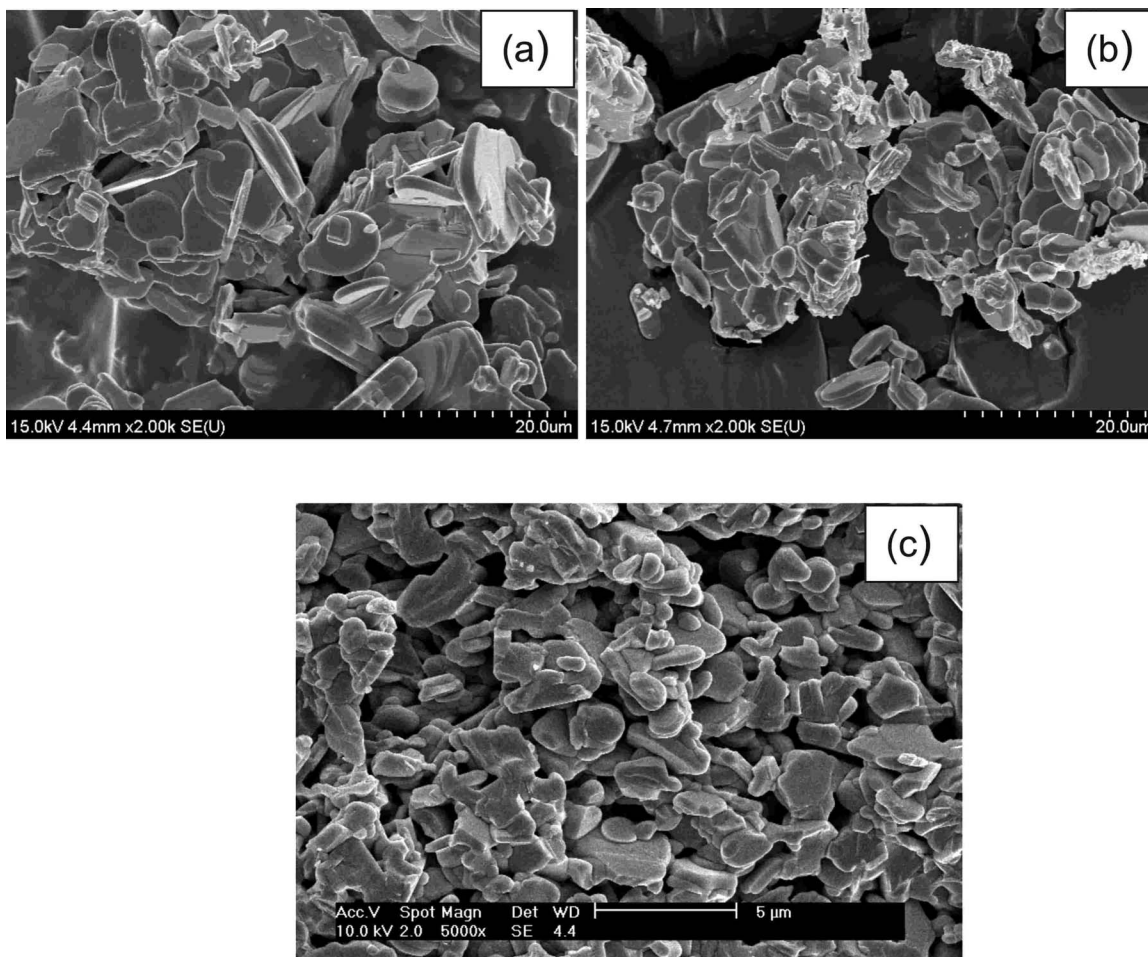


FIG. 4. Microstructure of (a) CBT, (b) SBT, and (c) BBT powders calcined at 950 °C.

gested that this orthorhombic structure is due to the combination of rotation of TiO_6 , resulting from less than optimal size of the A -type cation, and displacement of the Ti atoms toward the Bi_2O_2 layers. They also observed a partial disorder of the Bi and A -type cations in two out of the three available sites, which increases with the increase in the radius of the A site cation.

Figure 4 shows the SEM micrograph of different ceramics prepared through this modified chemical route. The figure shows a platelike grain structure. It is also found from the SEM micrograph that the grains of different sizes are homogeneously distributed.

Figures 5–7 show the temperature dependent dielectric properties (permittivity and dielectric loss) of ceramics in a fixed frequency format. It was found that the compounds CBT (Fig. 5) and SBT (Fig. 6) have frequency independent transition temperatures at 787 and at 525 °C, respectively, indicating the occurrence of normal ferroelectric–paraelectric phase transitions. Above the transition temperature permittivity follows the Curie–Weiss law. For the BBT compound, (Fig. 7) the dielectric anomaly is quite broad, covering the temperature range over 250 °C. This compound exhibits diffuse dielectric constant anomalies around T_m . It can be also noticed that, for BBT ceramic, the maximum of dielectric permittivity ϵ_m and the corresponding temperature maximum, T_m , depend on the measurement frequencies. The mag-

nitude of the dielectric constant decreases with an increase in frequency, and the maximum shifts toward higher temperature. This indicates that the dielectric polarization is of relaxation type in nature. The empirical relaxation strength describing the frequency dispersion of T_m , defined as $\Delta T_{\text{res}} = T_{m(1 \text{ MHz})} - T_{m(10 \text{ kHz})}$, is found to be 16.01 for BBT ceramic. Similar ferroelectric phase transitions have been re-

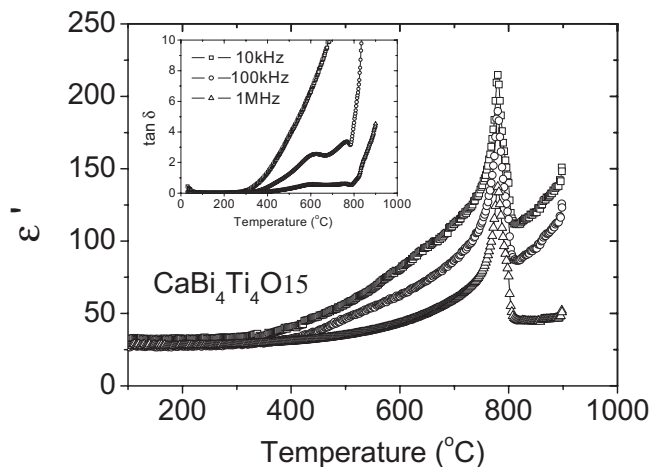


FIG. 5. Variation of dielectric constant (ϵ') of CBT ceramic as a function temperature; inset shows the temperature dependency of dielectric loss ($\tan \delta$).

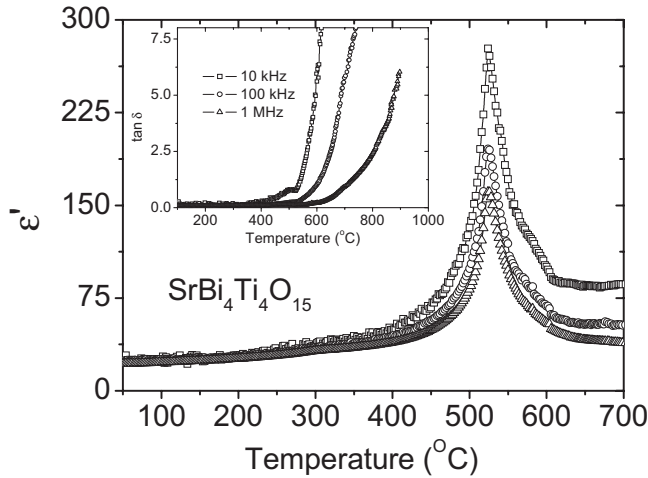


FIG. 6. Variation of dielectric constant (ϵ') of SBT ceramic as a function temperature; inset shows the temperature dependency of dielectric loss ($\tan \delta$).

ported in these compounds prepared by standard ceramic process.^{22–24} The observed dielectric constants are in the same range as that observed by Subbarao.²⁵ Usually ferroelectrics with a large ionic displacement have a high Curie temperature, a large spontaneous polarization, and a large coercive field. The ionic displacements are influenced by several factors including the ionic size, tolerance factor, and ionic polarizability. Considering the average ionic radii of the A site cation, the perovskite tolerance factors, $t = (R_A + R_O) / \sqrt{2(R_B + R_O)}$, are found to be 0.957, 0.968, and 0.989 for CBT, SBT, and BBT, respectively, which supports the cation disorder and phase transitions study by synchrotron x-ray and neutron powder diffraction data.²¹ The increase in transition temperature by decreasing A site cationic size ($\text{Ba}^{2+} > \text{Sr}^{2+} > \text{Ca}^{2+}$) is consistent with Subbarao's suggestion.²⁵ When in a lattice, which is restricted by rigid Bi_2O_2 layers, the substitution of A site ion with larger radii reduces the rattle space for B site ion is reduced. This result may reduce the transition temperature. On the other side, in CBT ceramic, when smaller radius Ca is placed in 12 coordination sites, it traps eight near neighbor oxygen and four

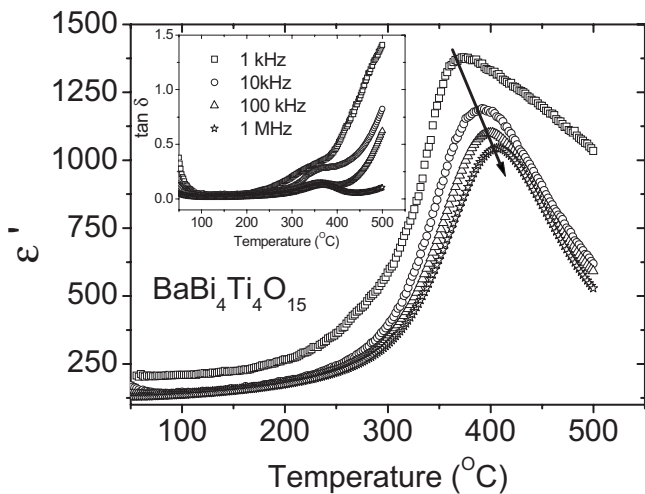


FIG. 7. Variation of (a) dielectric constant (ϵ') and (b) dielectric loss ($\tan \delta$) of BBT ceramic as a function temperature.

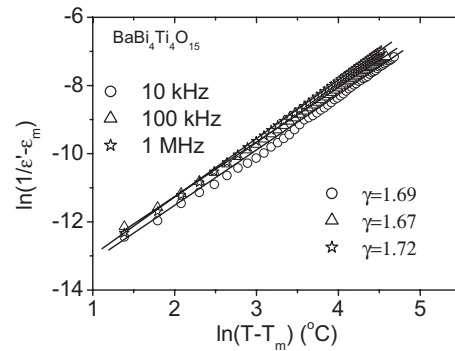


FIG. 8. $\log(1/\epsilon' - 1/\epsilon_m)$ vs $\log(T - T_m)$ for $\text{BaBi}_4\text{Ti}_4\text{O}_{15}$ at different frequencies.

more distant ones. This modification suggests a possible displacement of Ca^{2+} out of the oxygen dodecahedron center to induce a dipolar moment whose occurrence may lead to increase in transition temperature.

The dielectric losses of the samples (insets of Figs. 5–7) at low temperature appear to be stable but sensitive at high temperatures. The higher value of $\tan \delta$ at high temperatures may be due to transport of ions with higher thermal energy. The sharp increase in $\tan \delta$ may be due to the scattering of thermally activated charge carriers and some defects in the samples. At higher temperature the conductivity begins to dominate, which in turn is responsible for the rise in $\tan \delta$ (that is associated with the loss by conduction (i.e., $\sigma \propto \tan \delta$)). Also at high temperature (paraelectric phase) the contribution of ferroelectric domain walls to $\tan \delta$ decreases, which is responsible for the rise in $\tan \delta$. These types of dielectric behavior were also observed in some similar types of compounds.²⁶ The observed dielectric loss in BBT ceramic are less than that observed by Hou *et al.*²⁴ This may be due to the lower defect in the crystals, synthesized by this modified chemical route.

A generalized semiempirical relation has been applied to describe the phase transition modes of a relaxor-type BBT compound as

$$\frac{1}{\epsilon'} - \frac{1}{\epsilon_m} = (T - T_m)^\gamma / C,$$

where γ and C' are assumed to be constant. The parameter γ gives information on the character of the phase transition. $\gamma = 1$, a normal ferroelectric–paraelectric phase transition, and $\gamma = 2$ refers to ideal relaxors with a complete diffuse phase transition. The plots of $\log(1/\epsilon' - 1/\epsilon_m)$ versus $\log(T - T_m)$ at three different frequencies are shown in Fig. 8. The slopes of the fitting curves are used to determine the value of the parameter γ . The observed values of γ refer to the medial state between relaxor and normal ferroelectrics.

In order to analyze the relaxation feature of the ceramic frequency dependent T_m is shown in Fig. 9. The experimental curves were fitted (solid line) using the Vogel–Fulcher (VF) formula²⁷

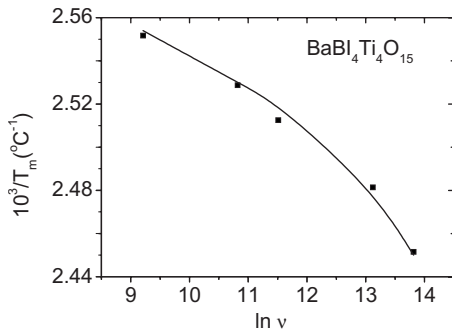


FIG. 9. Frequency dependency of $1/T_m$ for BBT ceramic. The circles are the experimental points and the line fits to the VF relationship.

$$\nu = \nu_o \exp \left[\frac{-E_a}{k_B(T_m - T_f)} \right],$$

where ν_o is the attempt frequency, E_a is the measure of average activation energy, k_B is the Boltzmann constant, and T_f is the freezing temperature. T_f is regarded as the temperature where the dynamic reorientation of the dipolar cluster polarization can no longer be thermally activated. The fitting parameters are $E_a=0.02$ eV, $\nu_o=5.79 \times 10^{11}$ Hz, and $T_f=362$ °C. The close agreement of the data with the VF relationship suggests the relaxor behavior in the system. The observed freezing temperature T_f below the Curie temperature, being dictated by random bond fluctuations, indicates a transformation into the ferroelectric long range order state on cooling. Here the activation energy and pre-exponential factor are both consistent with thermally activated polarization fluctuations.

The relaxor behavior as observed in this ceramic can be induced by many reasons, such as microscopic composition fluctuation, the merging of micropolar regions into macropolar regions, or a coupling of order parameter and local disorder mode through the local strain. Vugmeister and Glinchuk reported that the randomly distributed electrical strain field in a mixed oxide system is the main reason leading to the relaxor behavior.²⁸ As no macroscopic phase separation exists in the studied ceramic, we cannot exclude chemical heterogeneity in nanoscale. The distortion arising in the oxygen octahedra, a redistribution of the charge, and local formation of charge center result may be the sources of random field. This kind of random field is much weaker than that stemming from heterovalent cation substitution as in conventional relaxors. Hence, at high temperature, the strength of random field-fluctuating dipole moments of the individual unit cell can give rise to polar nanoregions. Here the polar correlations are strongly diminished and polar domains are less likely to nucleate.

The study of BBT crystal has proved a stable spontaneous polarization and orthorhombic structure below T_m .^{18,29} On the other hand, the observed shift of T_m [Fig. 7(a)] with measuring frequency suggests the existence of polar clusters in BBT. To explain this, one must understand the cation disorder in the Ba based bismuth layered structure compounds. At the first glance on the formula, one could expect that the BBT has no cation disorder, as each site seems to be occupied by only one kind of cation. A site bismuth has proved to

contribute much to the ferroelectricity in Bi layered structure compounds.^{30,31} Regarding the $\text{BaBi}_4\text{Ti}_4\text{O}_{15}$ phase, most of the previous crystallographic studies^{32,33,18} have demonstrated the necessity to partially substitute Bi for Ba in the $[\text{Bi}_2\text{O}_2]$ slabs to account for the experimental diffraction data. Actually most of the Aurivillius phases possess atomic positions with a mixed occupancy (on the A and/or B site of the perovskite blocks) without being associated with a relaxor behavior. Kennedy *et al.*²¹ observed a partial disorder of the Bi and A-type cations over two out of the three available sites, which is maximum for Ba and minimum for Ca in $\text{ABi}_4\text{Ti}_4\text{O}_{15}$ ceramics. Tellier *et al.*³⁴ showed a distinct positional (among Ba and Bi ions) and static disorder in the BBT composition. Such disorder may associate with the ferroelectric relaxor behavior through the formation of local charge center in the microdomains of BBT ceramics. In addition, the cation redistribution also leaves positive point charges on perovskite slabs where Bi^{3+} replaces Ba^{2+} and negative point charges in $(\text{Bi}_2\text{O}_2)^{2+}$ layers where Ba^{2+} replaces Bi^{3+} . These point charges result in an inner electric field along the c axis, which would destroy the long range polar ordering in BBT. Thus there are only short range polar clusters with a low concentration existing in the paraelectric matrix. In such a case, the interaction among these polar clusters is very weak, and the growth of polar clusters would be difficult on cooling or under an external electric field, which leads to relaxor behavior in the BBT ceramic. The random field caused by the cation redistribution can result in some polar clusters existing in the macrodomain of BBT, but it is not strong enough compared with the mean electric field to destroy completely the long range electric ordering in the composition. Thus, a real paraelectric-ferroelectric transition occurs on zero field cooling, although weak relaxor behaviors can be found in BBT.

IV. CONCLUSIONS

Aurivillius phase compounds, $\text{ABi}_4\text{Ti}_4\text{O}_{15}$ ($A=\text{Ca}$, Sr , and Ba), were synthesized by a modified chemical route, precipitating respective nitrate onto the surface of TiO_2 particles. XRD study showed that all compounds have orthorhombic symmetry at room temperature. SEM micrographs confirmed the platelike grain. Temperature dependent dielectric study revealed that the CBT and SBT ceramics exhibit sharp transition (normal ferroelectric behavior) at 787 and 525 °C, respectively, whereas BBT showed a broad phase transition (relaxorlike ferroelectric behavior). Regarding the normal phase transition in CBT and SBT, in agreement with tolerance factor, a significant deformation of the perovskite block was observed. For BBT ceramics, the quantitative characterization and comparison of relaxor behavior based on empirical parameters (γ and ΔT_{res}) confirmed its relaxorlike phase transition. The presence of a significant amount of foreign cations into the $[\text{Bi}_2\text{O}_2]$ slabs such as Ba^{2+} for $\text{BaBi}_4\text{Ti}_4\text{O}_{15}$, the incompatibility between the Ba^{2+} anionic environment, and the configuration of the $[\text{Bi}_2\text{O}_2]$ slabs become more subtle, and at a local scale the continuity of the $[\text{Bi}_2\text{O}_2]$ slabs cannot be ensured. Existences of such faults or

mismatch in the layers stacking within the crystal may be the major cause for the observed relaxor behavior in BBT ceramic.

ACKNOWLEDGMENTS

S. K. Rout is pleased to acknowledge Department of Science and Technology, Government of India, New Delhi, for providing financial support through BOYSCAST post-doctoral fellowship. The research is jointly supported through Brian Korea 21 (BK21) project and Center for Ultramicrochemical Process Systems (CUPS) sponsored by KOSEF, Republic of Korea.

- ¹C. A. P. de Araujo, J. D. Cucharo, L. D. Mc Millan, M. C. Scott, and J. F. Scoll, *Nature (London)* **374**, 627 (1995).
- ²H. B. Park, B. S. Kang, S. D. Bu, T. W. Noh, J. Lee, and W. Joe, *Nature (London)* **401**, 682 (1999).
- ³L. A. Reznichenko, O. N. Razumovskaya, L. A. Shilkina, and N. V. Der-gunova, *Inorg. Mater.* **32**, 474 (1996).
- ⁴A. Z. Simões, C. S. Riccardi, M. A. Ramírez, L. S. Cavalcante, E. Longo, and J. A. Varela, *Solid State Sci.* **9**, 756 (2007).
- ⁵X. Zheng, X. Huang, and C. Gao, *J. Rare Earths* **25**, 168 (2007).
- ⁶J. Zeng, Y. Li, Q. Yang, X. Jing, and Q. Yin, *J. Eur. Ceram. Soc.* **25**, 2727 (2005).
- ⁷A. Z. Simões, M. A. Ramírez, A. H. M. Gonzalez, C. S. Riccardi, A. Ries, E. Longo, and J. A. Varela, *J. Solid State Chem.* **179**, 2206 (2006).
- ⁸P. Ferrer, J. E. Iglesias, and A. Castro, *Chem. Mater.* **16**, 1323 (2004).
- ⁹M. V. Gelfuso, D. Thomazini, and J. A. Eiras, *J. Am. Ceram. Soc.* **82**, 2368 (1999).
- ¹⁰Y. Noguchi, M. Miyayama, and T. Kudo, *Appl. Phys. Lett.* **77**, 3639 (2000).
- ¹¹A. Varma and J. P. Lebrat, *Chem. Eng. Sci.* **47**, 2179 (1992).
- ¹²C. H. Lu and C. H. Wu, *J. Eur. Ceram. Soc.* **22**, 707 (2002).
- ¹³S. K. Rout, T. Badapanda, E. Sinha, S. Panigrahi, P. K. Barhai, and T. P. Sinha, *Appl. Phys. A: Mater. Sci. Process.* **91**, 101 (2008).
- ¹⁴J. Bera and D. Sarkar, *J. Electroceram.* **11**, 131 (2003).
- ¹⁵Standard CCP-14 program CHECKCELL, see <http://www.ccp14.ac.uk/tutorial/lmgp/>.
- ¹⁶C. H. Hervoches, A. Snedden, R. Riggs, S. H. Kilcoyne, P. Manuel, and P. Lightfoot, *J. Solid State Chem.* **164**, 280 (2002).
- ¹⁷A. V. Murugan, A. B. Gaikwad, V. Samuel, and V. Ravi, *Ceram. Int.* **33**, 569 (2007).
- ¹⁸B. J. Kennedy, Y. Kubotab, B. A. Hunter, Ismunandar, and K. Kato, *Solid State Commun.* **126**, 653 (2003).
- ¹⁹B. Aurivillius, *Ark. Kemi* **1**, 463 (1949).
- ²⁰H. Irie, M. Miyayama, and T. Kudo, *J. Appl. Phys.* **90**, 4089 (2001).
- ²¹B. J. Kennedy, Q. Zhou, Ismunandar, Y. Kubota, and K. Kato, *J. Solid State Chem.* **181**, 1377 (2008).
- ²²X. Zheng, X. Huang, and C. Gao, *J. Rare Earths* **25**, 168 (2007).
- ²³R. Q. Chu, Z. J. Xu, Z. G. Zhu, G. R. Li, and Q. R. Yin, *Mater. Sci. Eng., B* **122**, 106 (2005).
- ²⁴R. H. Hou, X. M. Chen, and Y. W. Zeng, *J. Am. Ceram. Soc.* **89**, 2839 (2006).
- ²⁵E. C. Subbarao, *J. Phys. Chem. Solids* **23**, 665 (1962).
- ²⁶A. Fouskova and L. E. Cross, *J. Appl. Phys.* **41**, 2834 (1970).
- ²⁷D. Viehland, S. J. Jang, L. E. Cross, and M. Wutting, *J. Appl. Phys.* **68**, 2916 (1990).
- ²⁸B. E. Vugmeister and M. D. Glinchuk, *Rev. Mod. Phys.* **62**, 993 (1990).
- ²⁹T. Kobayashi, Y. Noguchi, and M. Miyayama, *Jpn. J. Appl. Phys., Part 1* **43**, 6653 (2004).
- ³⁰A. L. Kholkin, M. Avdeev, M. E. V. Costa, J. L. Bapista, and S. N. Dorogovtsev, *Appl. Phys. Lett.* **79**, 662 (2001).
- ³¹R. L. Withers, J. G. Thompson and A. D. Rae, *J. Solid State Chem.* **94**, 404 (1991).
- ³²G. Nalini and T. N. Guru Row, *Bull. Mater. Sci.* **4**, 275 (2002).
- ³³M. E. Fuentes, A. Mehta, L. Lascano, H. Camacho, R. Chianelli, J. F. Fernandez, and L. Fuentes, *Ferroelectrics* **269**, 159 (2002).
- ³⁴J. Telier, Ph. Boullary, M. Manier, and D. Mercurio, *J. Solid State Chem.* **77**, 1829 (2004).